Fluorine-Induced Chiral Coordination Arrays Containing Helical Hydrogen-Bonding Chains of Water or Fluorinated Ligand

ARTICLE *in* CRYSTAL GROWTH & DESIGN · DECEMBER 2011

Impact Factor: 4.89 · DOI: 10.1021/cg200902g

6 AUTHORS, INCLUDING:

Zhi-Hui Zhang
Changzhou University
72 PUBLICATIONS **1,432** CITATIONS
SEE PROFILE

Sheng-Chun Chen
Changzhou University
60 PUBLICATIONS **503** CITATIONS
SEE PROFILE

Qun Chen
58 PUBLICATIONS **506** CITATIONS
SEE PROFILE

Miao Du
Tianjin Normal University
307 PUBLICATIONS **9,110** CITATIONS
SEE PROFILE

CRYSTAL GROWTH & DESIGN

COMMUNICATION

pubs.acs.org/crystal

Fluorine-Induced Chiral Coordination Arrays Containing Helical Hydrogen-Bonding Chains of Water or Fluorinated Ligand

Zhi-Hui Zhang,[†] Sheng-Chun Chen,[†] Ming-Yang He,[†] Chao Li,[†] Qun Chen,[*,†] and Miao Du[*,‡]

[†]Key Laboratory of Fine Petrochemical Technology, Changzhou University, Changzhou 213164, P. R. China

[‡]College of Chemistry, Tianjin Key Laboratory of Structure and Performance for Functional Molecule, Tianjin Normal University, Tianjin 300387, P. R. China

Supporting Information

ABSTRACT: Two chiral d^{10} metallosupramolecular systems based on an achiral fluorinated Schiff-base ligand have been prepared and characterized. The Zn^{II} complex **1** reveals 2_1 helical coordination chains with the inclusion of rare water chains of opposite helix in the perpendicular channels, whereas the Cd^{II} complex **2** displays the homochiral 1D coordination motifs with 3_1 symmetry and a 3D supramolecular architecture built by C−H···F interactions.

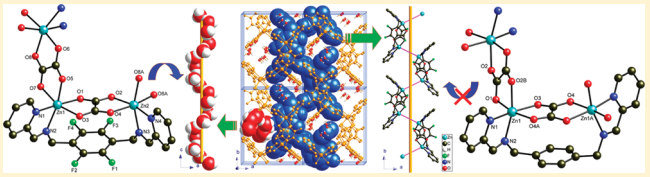

Due to the strong electronegativity and relatively small steric effect of fluorine, the replacements of hydrogen atoms with fluorine substituents in organic compounds have repeatedly attracted considerable attention.[1] In contrast to the previous reagents, fluorinated tectons have scarcely been explored in the aspect of inorganic−organic hybrids, especially metal−organic frameworks (MOFs) or coordination polymers, which in the last decades without doubt serve as novel materials not only in gas storage[2] but also in separation, catalysis, ion exchange, sensors, optoelectronics or photovoltaics, and drug release.[3] Fluorinated molecules are expected to possess superacidity, enhanced hydrophobicity, exceptional chemical and biological inertness, and excellent optical/electrical properties compared with their nonfluorinated counterparts.[4] Consequently, the introduction of fluorine into coordination assemblies may readily adjust the resulting coordination arrays, the host organizations, and the possible included cavities.

Recently, Omary and co-workers have reported the creation of the breathable porous crystalline coordination matrices with high density gas uptake and extraordinary hysteretic sorption of H_2 by the deliberate choice of a trifluoromethyl-substituted triazolate linker.[5] Inspired by the excellent gas adsorption ability of fluorous metal−organic frameworks (FMOFs),[5] we have initiated the study of dipyridyl fluorinated ligands and the associated supramolecular FMOFs derived from different metal centers. Remarkable entangled nets in coordination systems with both self-penetrating and interpenetrating structural features[6] have been constructed for the first time on the basis of a flexible fluorinated bis-pyridinecarboxamide ligand. The structural feature of MOFs is highly sensitive to the functional groups attached at the organic linkers. When covalently bound to the aromatic ring, halogen atoms are confirmed to be the versatile assembly organizing factors that direct the extended networks and induce the helical aggregation of Cu^{II} complexes.[7] As a result, the conformational freedom of the flexible fluorinated modules may provide a good opportunity for the construction of unusual coordination frameworks.

Meanwhile, considerable attention has been paid to supramolecular architectures with helices because of their important relevance to the functions of biological systems, optoelectronic materials, and chemical processes.[8−10] But to control the chirality and helicity at the supramolecular level is one of the major challenges in the design and synthesis of helical structures.[11] Besides enantioselective synthesis and by using racemic ligands to assemble with metal ions, the spontaneous resolution induced by the local distortion of achiral flexible ligands is an effective route to achieve such chiral crystalline materials.[12] It has also been found that noncovalent interactions, such as hydrogen bonds, halogen bonds, and $\pi-\pi$ interactions, may play a key role in the process of spontaneous resolution.[13] So our strategy is to use a flexible Schiff-base ligand with a fluorinated backbone as the building block. In this work, we present the synthesis of 2,3,5,6-tetrafluoro-1,4-bis(2-pyridylmethyleneaminomethyl)benzene (L_1) and its complexation with d^{10} metal ions to construct two intriguing species $\{[Zn_2(L_1)(oxa)_2]\cdot(H_2O)_4\}_n$ (**1**) and $[Cd(L_1)_{0.5}(Cl)(oxa)_{0.5}]_n$ (**2**) (oxa = oxalate), displaying novel 1D helical motifs with chiral water chains of O−H···O interactions or fluorinated ligand chains of weak C−H···F interactions, respectively. Significantly, when an analogous nonfluorinated ligand 1,4-bis(2-pyridylmethyleneaminomethyl) benzene (L_2) was used, a 1D zigzag chain of $\{[Zn_2(L_2)(oxa)_2]\cdot(H_2O)\}_n$ (**1a**) was obtained without any peculiarity of helix.

Received: July 15, 2011
Revised: September 28, 2011
Published: October 10, 2011

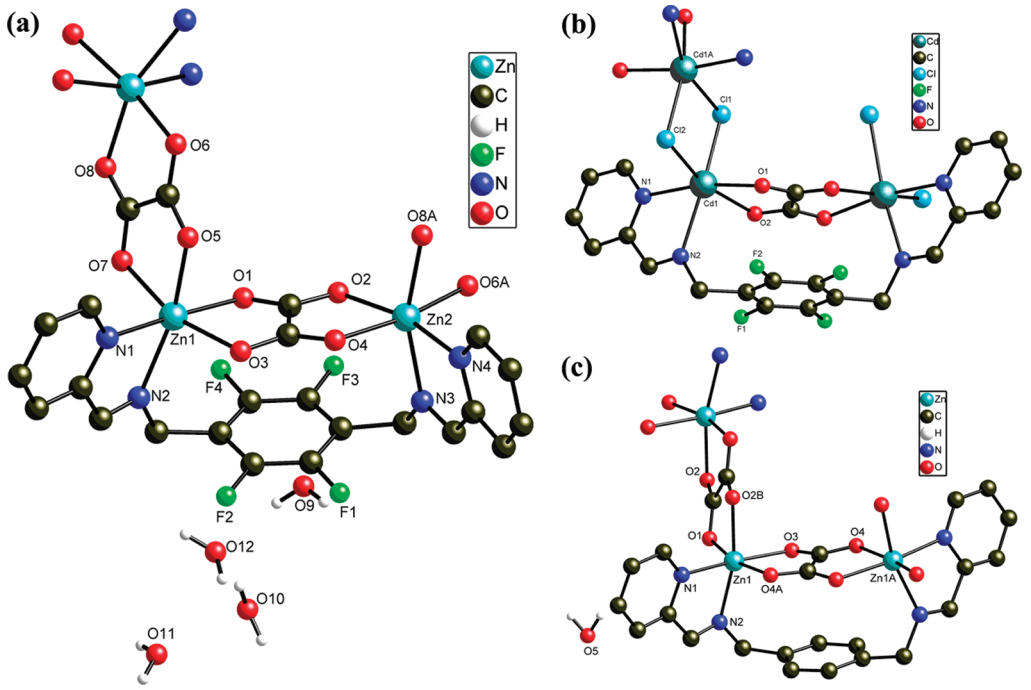

Figure 1. Coordination environments of Zn^{II} in **1** (a), Cd^{II} in **2** (b), and Zn^{II} in **1a** (c), with partial atom numbering schemes (symmetric codes for **1**: (A) $-x+2, y+{}^{1}/_{2}, -z+{}^{3}/_{2}$; symmetric codes for **2**: (A) $y, x, -z+2$; symmetric codes for **1a**: (A) $-x+1, y, -z+{}^{1}/_{2}$; (B) $-x+{}^{1}/_{2}, -y+{}^{1}/_{2}, -z$.).

The hydrothermal reaction[14] of $ZnCl_2 \cdot 6H_2O$ or $CdCl_2 \cdot 6H_2O$, L_1, and oxalamide yields colorless crystals of **1** or **2**, respectively, coming with the in situ formation of oxalate (oxa) anions. Whereas the fluorous ligand L_1 was replaced by non-fluorous molecule L_2, Zn^{II} complex **1a** was prepared as colorless single crystals under the same conditions.[14] Unfortunately, several efforts to prepare the Cd^{II} complex of L_2 failed. Notably, oxalamide was converted to oxalate by enduring an in situ reaction[15] in the preparation of the helical or zigzag architectures. All of the samples are insoluble in water and common organic solvents. The purities of them were confirmed by powder X-ray diffraction (PXRD) analyses, in which the experimental data of them are consistent with the single-crystal-simulated spectra, respectively (Figure S1 in the Supporting Information). The formulas of **1**, **2**, and **1a** were further confirmed by elemental analysis and TGA (see Figure S2 of the Supporting Information). The TGA study of **1** indicates the loss of water molecules in the temperature range of 105−185 °C; the weight loss (10.1%) is consistent with the calculated (9.4%) value. For **2**, the ligand molecules start to release at *ca.* 300 °C. While complex **1a** shows a weight loss of 3.6% from 45 to 115 °C, corresponding to the release of free water molecules (calcd: 2.8%). The decompositions of the remaining frameworks begin at 305 and 320 °C for **1** and **1a**, respectively.

Crystallographic analysis[16] shows that complex **1** crystallizes in the orthorhombic acentric space group $P2_12_12_1$ with the flack parameter of 0.014(6). In the 3D lattice, the polymeric Zn^{II} strings are wound to a rope with M (left-handed) configuration. The asymmetric unit is composed of one $[(Zn_2)(L_1)(oxa)_2]$ motif and four lattice water molecules. As depicted in Figure 1a, each crystallographically independent Zn1 or Zn2 ion takes a slightly distorted octahedral coordination geometry provided by four O atoms from two oxa ligands and two N donors from the same side of one L_1 ligand. The Zn−O bond distances range from 2.0899(15) to 2.1294(15) Å, and the Zn−N lengths range from 2.1237(17) to 2.2149(17) Å, similar to those observed in other Zn^{II} Schiff-base complexes.[17] The bond angles around Zn^{II} centers range from 79.28(6) to 170.41(6)°. Within the tetradentate chelating L_1 ligand, two 2-pyridyl groups are nearly perpendicular (ca. 89°) to the central substituted benzene ring at the same side to benefit its *gauche*-configuration, with the dihedral angles between themselves of 80.09(5)°. Both oxalate ligands take the chelating−bridging coordination mode. One of them connects two Zn^{II} ions that are chelated by the same L_1

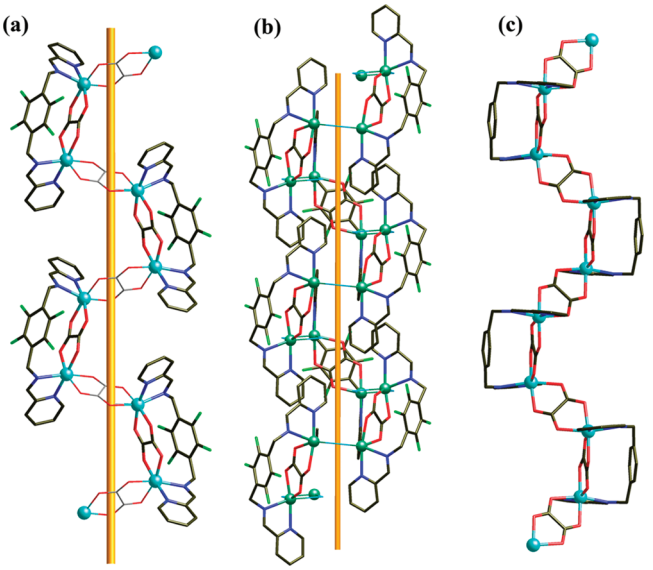

Figure 2. 1D helix of (a) **1** and (b) **2** and the 1D zigzag chain of (c) **1a**.

dx.doi.org/10.1021/cg200902g |*Cryst. Growth Des.* 2011, 11, 5171–5175

ligand to form a $[(Zn_2)(L_1)(oxa)]$ dinuclear unit. The other oxalate joins the adjacent dinuclear units to afford an infinite 1D array, which shows an M-helix along the 2_1 screw axis at $[1, y, {}^3/_4]$ with a pitch of 15.006(3) Å (see Figure 2a).

A detailed analysis shows that there are no obvious hydrogen-bonding and $\pi-\pi$ interactions between neighboring strands. However, the chirality of the originally formed 1D helical chain is transferred to an adjacent chain through the complementary interchain hydrophobic interactions, resulting in a second chain with the same chirality. Each chain connects to four adjacent chains through the interchain hydrophobic interactions (Figure S3 in the Supporting Information) to generate narrow channels with M-helices along the *a* axis. Within each chiral channel, a 1D right-handed (P) chiral water chain is formed around the 2_1 axis parallel to the *a* axis (Figure 3, left). Multiple O−H···O interactions are found to stabilize the well-defined water chain (Table S5 of the Supporting Information). Each hydrogen-bonded chiral water chain further connects the adjacent two chiral 1D coordination motif via O10−H10A···O2 bonds to yield a final 3D host−guest supramolecular architecture.

Colorless prism crystals of **2** crystallize in the chiral trigonal space group $P3_12_1$ with the flack parameter of 0.011(18). The fundamental building units consist of one Cd^{II} ion; one L_1 ligand and one oxalate, both lying on the same 2-fold axis; as well as a bridging chlorine anion (see Figure 1b). The Cd1 ion takes an octahedral geometry, which is six-connected by two nitrogen atoms from L_1, two oxygen atoms from oxalate, and two chlorine ions. Meanwhile, each L_1 ligand coordinates to two Cd^{II} centers with the combination of one chelating−bridging oxalate ligand to form a $[(Cd_2)(L_1)(oxa)]$ dinuclear unit, which is similar to that in **1** but has a 2-fold axis passing through the center of the tetrafluorinated benzene ring of the L_1 and the midpoint of the C−C bond of oxalate. The dihedral angle between the two terminal 2-pyridyl groups within the L_1 ligand is about 2.57(9)°. The above-mentioned dinuclear units are further extended by double chloride bridging to generate an infinite single helical chain with P (right-handed) configuration along the [001] axis with the pitch of 12.3392(10) Å (see Figure 2b). Interestingly, significant parallel $\pi-\pi$ interactions are found between two terminal pyridyl rings of adjacent dinuclear units in a single helix, with the center to center distance of 3.455(2) Å. All helical chains are running along the 3_1 screw axis in an interlocked fashion, resulting in a 3D homochiral supramolecular lattice, in which the halogen atoms (F2 and Cl2) are involved in various hydrogen bonding interactions (see Figure 4b). The methylene group of L_1 is H-bonded to the F2 atom from the neighboring L_1 ligand (C7−H7B···F2) to afford a helical H-bonding chain with right-handedness (P-configuration), as indicated in Figure 4c. In addition, the C6−H6···Cl2 interactions further stabilize the 3D homochiral supramolecular array.

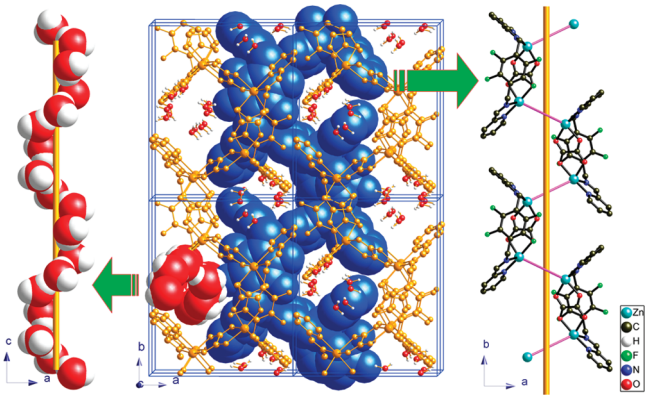

Figure 3. 3D supramolecular framework of **1** with 1D left-handed helical channels occupied by 1D right-handed water chains. (Left) The single helical water chain is highlighted in space-filling mode. (Right) Single helical coordination chain with one of the two oxalate ligands highlighted as a purple linker for clarity.

When a nonfluorinated ligand L_2, instead of L_1, was used to react with zinc chloride and oxalamide, it is interesting to find that the resulting complex **1a** crystallizes in the centrosymmetric space group *C*2/*c*. There is one Zn^{II} center, one L_2 ligand lying on the 2-fold axis of $[{}^1/_2, y, {}^1/_4]$, two centrosymmetric oxa anions, and one lattice water in the asymmetric unit. The six-coordinated Zn^{II} ion is surrounded by two N atoms from the chelating L_2 ligand and four O atoms from two oxalate anions, respectively. The coordination geometry of Zn1 in **1a** is very similar to that in **1** and can also be described as a distorted octahedral $[ZnN_2O_4]$ (Figure 1c). The Zn−N/Zn−O bond lengths are in good agreement with those observed in complex **1**. Unlike in **1**, the bis-chelating L_2 ligand combines with the μ_2-bridging oxalato ligands to fulfill a zigzag $[(Zn_2)(L_2)(oxa)_2]_n$

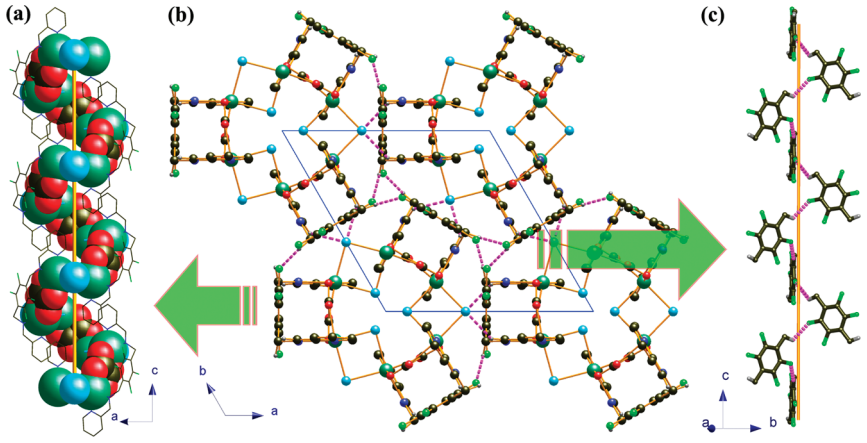

Figure 4. (a) Single helical coordination chain with the $[Cd_2Cl_2(oxa)]_n$ motif highlighted as a space filling mode for clarity. (b) Crystal packing of **2** viewed along the [001] direction, showing hydrogen bonds as dashed lines. (c) Perspective view of the 3_1 helix constructed by C−H···F interactions along the [001] direction.

dx.doi.org/10.1021/cg200902g |*Cryst. Growth Des.* 2011, 11, 5171–5175

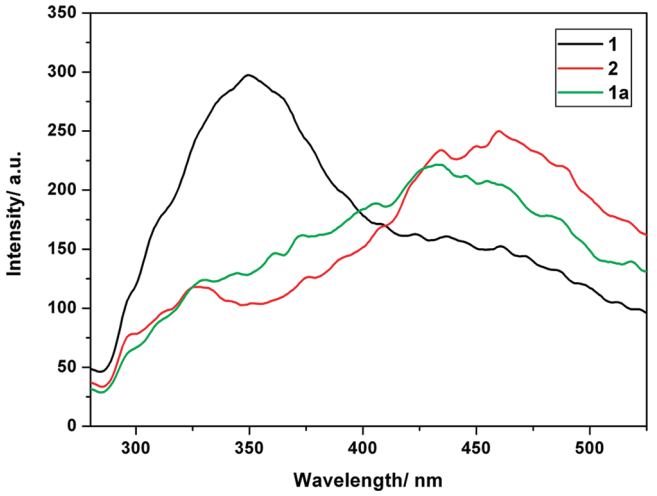

Figure 5. Solid state emission spectra of **1**, **2**, and **1a**.

chain of **1a** along the [101] direction (Figure 2c), which is anchored by lattice water moieties through O5−H5···O2 interactions. The adjacent 1D coordination arrays are further extended via the $\pi-\pi$ interactions between the terminal pyridyl rings [center to center distance, 3.633(4) Å; dihedral angle, 12.57(2)°]. Moreover, the C−H···O interactions between the adjoining 2D arrays in the parallel stacking mode result in the final 3D supramolecular arrangement of **1a** (see Figure S4 and Table S5 of the Supporting Information for details).

From the above discussion, the structural diversification of this series of polymeric complexes should be ascribed to the nature of the metal coordination as well as the subtle discrepancy of ligands (with or without fluorine substituents). Metal ions have similar coordination geometries in all three cases, and the same primary structure [$(M_2)(L)(oxa)$] (M = Zn in **1** and **1a**; M = Cd in **2**; L = L_1 in **1** and **2**; L = L_2 in **1a**) is also available. As for the ligands, the Schiff-base ligands with or without fluorine substituents all display the *gauche*-configuration, in which the two terminal 2-pyridyl groups provide the dihedral angles of 80.09(5), 2.57(9), and 12.56(2)° in **1**, **2**, and **1a**, respectively. Nevertheless, in comparison with **1a**, the chirality of the single crystal of **1** is evidently owing to the screw coordination arrangement of the achiral fluorinated ligand L_1 around the Zn^{II} centers. Further analyses of supramolecular structures in all three complexes indicate that the fluorine groups are involved in the weak interactions for both **1** and **2** (interchain hydrophobic interactions in **1** and C−H···F helical H-bonding chains in **2**), while C−H···O interactions between the benzene ring of nonfluorinated ligand L_2 and oxa O atoms are found to fulfill the 3D supramolecular network in **1a**. So the participation in supramolecular arrangements of fluorine substituents may give the explanation for the formation of helical architectures in **1** and **2**.

To explore their potential applications as luminescent crystalline materials, solid-state fluorescent properties for all complexes were studied at room temperature upon excitation at 272 nm (see Figure 5). The Zn^{II} complex **1** shows a broad emission from 290 to 415 nm with λ_{max} of 350 nm, which is luminescent in the purple region, while complexes **2** and **1a** display very broad blue emission bands with λ_{max} of 460 and 430 nm, respectively.

In summary, we have developed a novel approach to construct chiral coordination assemblies by using the achiral fluorinated-ligands as building blocks. To the best of our knowledge, complexes **1** and **2** represent the first examples of fluorinated groups inducing homochiral coordination systems. The slight change of the fluorinated and nonfluorinated ligands as well as the metal ions leads to the formation of remarkably distinct coordination architectures. It is also evident that the achiral fluorinated ligands tend to generate helical arrangements, and such Schiff-base type fluorinated ligands should be further systematically investigated for the development of novel chiral crystalline materials with potential applications in the future.

■ ASSOCIATED CONTENT

Supporting Information. Experimental details, PXRD patterns, TGA curves, additional structural diagrams and tables, and crystallographic data (CCDC 814075−814077) for all complexes. This material is available free of charge via the Internet at http://pubs.acs.org.

■ AUTHOR INFORMATION

Corresponding Author

*Q.C.: telephone and fax, 86-519-86330251; e-mail, chenqunjpu@yahoo.com. M.D.: telephone and fax, 86-22-23766556; e-mail, dumiao@public.tpt.tj.cn.

■ ACKNOWLEDGMENT

This work was financially supported by Jiangsu Province Outstanding Science and Technology Innovation Team and Changzhou University (ZMF 10020073). M.D. also acknowledges the financial support from the National Natural Science Foundation of China (No. 20971098) and Tianjin Normal University.

■ REFERENCES

(1) Nyffeler, P. T.; Gonzalez Durón, S.; Burkart, M. D.; Vincent, S. P.; Wong, C.-H. *Angew. Chem., Int. Ed.* **2005**, *44*, 192–212.

(2) (a) Frost, H.; Snurr, R. Q. *J. Phys. Chem. A* **2007**, *111*, 18794–18803. (b) Lee, T. B.; Kim, D.; Jung, D. H.; Choi, S. B.; Yoon, J. H.; Kim, J.; Choi, K.; Choi, S. H. *Catal. Today* **2007**, *120*, 330–335. (c) Rowsell, J. L. C.; Spencer, E. C.; Eckert, J.; Howard, J. A.; Yaghi, O. M. *Science* **2005**, *309*, 1350–1354.

(3) (a) Férey, G. *Chem. Soc. Rev.* **2008**, *37*, 191–214. (b) Fischer, R. A.; Wöll, C. *Angew. Chem., Int. Ed.* **2008**, *47*, 8164–8168.

(4) Gladysz, J. A., Curran, D. P., Horváth, I. T., Eds. *Handbook of Fluorous Chemistry*; Wiley/VCH: Weinheim: Germany, 2004.

(5) (a) Yang, C.; Wang, X.; Omary, M. A. *Angew. Chem., Int. Ed.* **2009**, *48*, 2500–2505. (b) Yang, C.; Wang, X.; Omary, M. A. *J. Am. Chem. Soc.* **2007**, *129*, 15454–15455.

(6) Zhang, Z.-H.; Chen, S.-C.; Mi, J.-L.; He, M.-Y.; Chen, Q.; Du, M. *Chem. Commun.* **2010**, 8427–8429.

(7) Zhang, F.; Yajima, T.; Li, Y. Z.; Xu, G. Z.; Chen, H. L.; Liu, Q. T.; Yamauchi, O. *Angew. Chem., Int. Ed.* **2005**, *44*, 3402–3407.

(8) (a) Lehn, J.-M. *Chem.—Eur. J.* **2000**, *6*, 2097–2102. (b) Seitz, M.; Kaiser, A.; Stempfhuber, S.; Zabel, M.; Reiser, O. *J. Am. Chem. Soc.* **2004**, *126*, 11426–11427. (c) Giuseppone, N.; Schmitt, J.-L.; Lehn, J.-M. *J. Am. Chem. Soc.* **2006**, *128*, 16748–16763.

(9) (a) Hirschberg, J. H. K. K.; Brunsveld, L.; Ramzi, A.; Vekemans, J. A.; Sijbesma, R. P.; Meijer, E. W. *Nature* **2000**, *407*, 167–170. (b) Kodama, K.; Kobayashi, Y.; Saigo, K. *Cryst. Growth Des.* **2007**, *7*, 935–939.

(10) (a) Seo, J. S.; Whang, D.; Lee, H.; Jun, S. I.; Oh, J.; Jeon, Y. J.; Kim, K. *Nature* **2000**, *404*, 982–986. (b) Lee, S. J.; Lin, W. *Acc. Chem. Res.*

2008, *41*, 521–537. (c) Hembury, G. A.; Borovkov, V. V.; Inoue, Y. *Chem. Rev.* **2008**, *108*, 1–72.

(11) Zheng, X.-D.; Lu, T.-B. *CrystEngComm* **2010**, *12*, 324–336.

(12) (a) Bu, X.-H.; Chen, W.; Du, M.; Biradha, K.; Wang, W.-Z.; Zhang, R.-H. *Inorg. Chem.* **2002**, *41*, 437–439. (b) Qu, Z.; Zhao, H.; Wang, Y.; Wang, X.; Ye, Q.; Li, Y.; Xiong, R.; Abrahams, B. F.; Liu, Z.; Xue, Z.; You, X. *Chem.—Eur. J.* **2004**, *10*, 53–60. (c) Zhang, J.; Yao, Y.; Bu, X. *Chem. Mater.* **2007**, *19*, 5083–5089. (d) Li, J.-R.; Tao, Y.; Yu, Q.; Xian, X.-H.; Sakamoto, H.; Kitagawa, S. *Chem.—Eur. J.* **2008**, *14*, 2771–2776. (e) Tong, X.-L.; Hu, T.-L.; Zhao, J.-P.; Wang, Y.-K.; Zhang, H.; Bu, X.-H. *Chem. Commun.* **2010**, *46*, 8543–8545.

(13) (a) Wang, Y. T.; Tong, M. L.; Fan, H. H.; Wang, H. Z.; Chen, X. M. *Dalton Trans.* **2005**, 424–426. (b) Balamurugan, V.; Mukherjee, R. *CrystEngComm* **2005**, *7*, 337–341.

(14) All complexes were similarly synthesized by a typical procedure as described for **1**. A mixture of $ZnCl_2 \cdot 6H_2O$ (24.4 mg, 0.1 mmol), L_1 (19.3 mg, 0.05 mmol), and oxalamide (8.8 mg, 0.1 mmol) was dissolved in H_2O (7 mL). The mixture was heated in a Teflon vessel for 24 h at 120 °C. After cooling of the vessel to room temperature at a rate of 5 °C·h^{-1}, colorless single crystals of **1** were collected.

(15) Oxamide can be converted to ammonium oxalate and oxalic acid by heating it for long periods with water.Riemenschneider, W.; Tanifuji, M. Oxalic Acid. *Ullmann's Encyclopedia of Industrial Chemistry*; 2000.

(16) Crystal data for **1**: orthorhombic, $P2_12_12_1$, a = 12.299(2) Å, b = 15.006(3) Å, c = 15.438(3) Å, γ = 120°, V = 2849.3(9) Å^3, Z = 4, ρ = 1.784 g/cm^3, μ = 1.781 mm^{-1}, R_1 = 0.0219, wR_2 = 0.0585. Crystal data for **2**: trigonal, $P3_12_1$, a = 13.0654(6) Å, b = 13.0654(6) Å, c = 12.3392(10) Å, V = 1824.16(19) Å^3, Z = 6, ρ = 2.103 g/cm^3, μ = 2.038 mm^{-1}, R_1 = 0.0149, wR_2 = 0.0367. Crystal data for **1a**: monoclinic, $C2/c$, a = 13.294(3) Å, b = 16.269(4) Å, c = 11.180(3) Å, β = 99.609(4)°, V = 2384.1(10) Å^3, Z = 4, ρ = 1.781 g/cm^3, μ = 2.077 mm^{-1}, R_1 = 0.0517, wR_2 = 0.0942.

(17) Dumitru, F.; Legrand, Y.-M.; Lee, A. V.; Barboiu, M. *Chem. Commun.* **2009**, 2667–2669.